(A) Title Page

Deficiency mutations of α_1-antitrypsin differentially affect folding, function and polymerization

Author affiliations:

Imran Haq[1,2,*], James A. Irving[1,2,*], Aarash D. Saleh[3], Louis Dron[3], Gemma L. Regan-Mochrie[1], Neda Motamedi-Shad[1,2], John R. Hurst[3], Bibek Gooptu[2,3,4,§] and David A. Lomas[1,2,3,§]

[1]Wolfson Institute for Biomedical Research, University College London, London, WC1E 6BN, UK
[2]Institute of Structural and Molecular Biology/Birkbeck, University of London, London, WC1E 7HX, UK
[3]London Alpha-1 Antitrypsin Deficiency Service, Royal Free Hospital, Pond Street, London, NW3 2QG, UK
[4]Division of Asthma, Allergy and Lung Biology, King's College London, London, SE1 9RT, UK

*Denotes equal contribution
§Joint senior authors

Short title:

Distinct properties of A336P and Z α_1-antitrypsin

Corresponding author:

Prof. David Lomas, University College London, 1st Floor, Maple House, 149 Tottenham Court Road, London W1T 7NF, UK

Tel: (+44) 020 7679 0876E-mail: d.lomas@ucl.ac.uk

Author contributions: I.H., J.A.I., J.R.H., B.G. and D.A.L. conceived and designed the study. I.H., J.A.I., A.D.S., L.D., G.L.R. and N.M. performed experiments/data acquisition. I.H., J.A.I., L.D., J.R.H., B.G. and D.A.L. analyzed and interpreted data. I.H., J.A.I., B.G. and D.A.L. wrote, and all authors edited and approved, the manuscript.

Funding information: This work was supported by the Medical Research Council (UK). I.H. is supported by GlaxoSmithKline. A.D.S. and D.A.L. are supported by the NIHR Biomedical Research Centre at University College London Hospitals NHS Foundation Trust and University College London. G.L.R. was the recipient of a Smith College "Praxis: The Liberal Arts at Work" summer internship. N.M. was supported by a Marie Curie Fellowship.

(B) Abstract

Misfolding, polymerization and defective secretion of functional α_1-antitrypsin underlies the predisposition to severe liver and lung disease in α_1-antitrypsin deficiency. We have identified a novel (Ala336Pro, Baghdad) deficiency variant and characterized it relative to the wild-type (M) and Glu342Lys (Z) alleles. The index case is a homozygous individual of consanguineous parentage, with levels of circulating α_1-antitrypsin in the moderate deficiency range, but a biochemical phenotype that could not be classified by standard methods. The majority of the protein was present as functionally inactive polymer, and the remaining monomer was 37% active relative to the wild-type protein. These factors combined indicate a 85-95% functional deficiency, similar to that seen with ZZ homozygotes. Biochemical, biophysical and computational studies further defined the molecular basis of this deficiency. These demonstrated that native Ala336Pro α_1-antitrypsin could populate the polymerogenic intermediate – and therefore polymerize – more readily than either wild-type α_1-antitrypsin or the Z variant. In contrast, folding was far less impaired in Ala336Pro α_1-antitrypsin than in the Z variant. The data are consistent with a disparate contribution by the 'breach' region and 'shutter' region of strand 5A to folding and to polymerization mechanisms. Moreover, the findings demonstrate that in these variants, folding efficiency does not correlate directly with the tendency to polymerize *in vitro* or *in vivo*. They therefore differentiate generalized misfolding from polymerization tendencies in missense variants of α_1-antitrypsin. Clinically they further support the need to quantify loss-of-function in α_1-antitrypsin deficiency to individualize patient care.

(C) Keywords

α_1-antitrypsin deficiency, polymerization, intermediate, mutation, protease inhibition, unfolding, refolding, serpinopathies

Abbreviations

AF488, Alexa Fluor 488; AF594, Alexa Fluor 594; CD, circular dichroism; COSM, centre of spectral mass; IEF, isoelectric focusing; k_{ass}, second-order association rate constant; PAGE, polyacrylamide gel electrophoresis; PBS, phosphate-buffered saline; SI, stoichiometry of inhibition.

(D) Text

Introduction

α_1-Antitrypsin is produced in the liver, circulates as the most abundant antiprotease, and critically regulates activity of neutrophil elastase and proteinase-3 in the lung. Its mechanism of action involves a transition from a metastable native state with a 5-stranded central β-sheet to a thermodynamically favored 6-stranded central β-sheet conformation. This metastability is subverted by pathogenic mutations in α_1-antitrypsin deficiency, one of the most common hereditary disorders. Over 120 mutations in the SERPINA1 gene encoding α_1-antitrypsin have been identified, with approximately 80 implicated in disease pathogenesis, indicative of a highly polymorphic gene (1). Current screening involves quantification of circulating levels, with M (wild-type; AT_M) homozygotes (PiMM) ranging between 1.0–2.8 g/L of α_1-antitrypsin (2); clinically-relevant deficiency is considered when levels are ≤0.5 g/L. Isoelectric focusing (IEF) of the plasma protein identifies variants by their migration patterns (3). Around 95% of clinically-significant deficiency is caused by the Z (Glu342Lys; AT_Z) pathogenic variant. Approximately 1 in 1600 individuals in populations of North European descent are homozygous for this allele (PiZZ), and in these individuals plasma levels are ≤0.2 g/L (4, 5). Misfolding of the Z α_1-antitrypsin polypeptide chain results in degradation (6), but is also associated with accumulation of α_1-antitrypsin molecules that have undergone aberrant stabilization through ordered self-association (polymerization). Polymers have a 'beads-on-a-string' appearance when viewed by electron microscopy (7) and are sequestered within inclusions in the endoplasmic reticulum (ER) of hepatocytes (8). Polymerization is associated with toxic gain-of-function and so predisposes to neonatal hepatitis, cirrhosis and hepatocellular carcinoma (9). The lack of circulating inhibitor permits excessive pulmonary inflammation, uncontrolled proteolytic degradation of lung parenchyma and hence severe panlobular emphysema, particularly in the context of smoking (10). These loss-of-function effects may be further aggravated by functional inactivation of α_1-antitrypsin by oxidative stress and polymerization of circulating protein (8, 11).

α_1-Antitrypsin adopts the conserved fold that is a hallmark of the serpin superfamily (12), comprising three β-sheets (A-C), nine α-helices (A-I) and a 'reactive centre loop' (RCL) bait sequence that acts as a pseudo-substrate for the target protease (Fig. 1A, *left*). Structural lability of the central β-sheet A is required for inhibitor function, but is also key to formation of ordered polymers. Here we describe a novel mutation affecting a central residue in β-sheet A, Ala336Pro, in a homozygous individual exhibiting a moderate deficiency of circulating α_1-antitrypsin. The novel variant (α_1-antitrypsin Baghdad; AT_{A336P}) has been investigated using immunological and biophysical approaches. The results show the individual to have a severe functional deficiency far beyond the reduction in plasma levels and that the homozygous state therefore confers comparable emphysema risk to that of PiZZ individuals. Additionally, the mutant provides mechanistic insight into the role of strand 5 of β-sheet A in the formation of the intermediate and subsequent steps in α_1-antitrypsin polymerization and the relationship between misfolding and polymerization.

Materials and Methods

Purification of α_1-antitrypsin and preparation of conformers

α_1-Antitrypsin was purified from human plasma using Alpha Select resin followed by Q Sepharose chromatography (GE Healthcare), and stored in phosphate-buffered saline (PBS), 5% v/v glycerol

and 0.17% v/v β–mercaptoethanol at -80°C. Wild-type (AT_M) protein purified in this way was indistinguishable from that obtained using previously published methods (13) when assessed by inhibitory activity, intrinsic tryptophan fluorescence, circular dichroism (CD) spectra or liquid chromatography mass spectroscopy (14).

Gel electrophoresis and western blot analysis

Plasma samples, diluted 1:100, were resolved by non-denaturing PAGE (polyacrylamide gel electrophoresis; Life Technologies) and transferred onto a PVDF membrane. Primary incubation was with the 2C1 antibody that specifically recognizes α_1-antitrypsin polymers (9) or a non-conformationally-selective rabbit polyclonal antibody against α_1-antitrypsin. The membrane was then washed and incubated with IR680RD anti-mouse or IR800CW anti-rabbit secondary antibodies with visualization using an Odyssey imaging system (LiCOR). All densitometry was performed using ImageJ (15). 8% w/v urea Tris-Glycine gels were produced using an SDS-free Laemmli system (16) with the addition of urea to 6M.

Assessment of proteinase inhibition

The stoichiometry of inhibition (SI) and association rate constant of α_1-antitrypsin (k_{ass}) were assessed at 25°C using bovine α-chymotrypsin as described previously (17). The ability to form an enzyme-inhibitor complex was assessed by incubating differing concentrations of protease with α_1-antitrypsin and resolution (without heating) by SDS-PAGE.

Spectral studies

Far-UV CD spectra were collected using a Jasco J-810 spectropolarimeter as described previously (17). Intrinsic fluorescence spectra (emission 300-400 nm) were collected using a Perkin Elmer LS50B spectrofluorimeter (excitation 280 nm, scan 500nm/s, 10 accumulations, 5nm slits). The centre of spectral mass (COSM) was calculated as a weighted average, with the intensity at each wavelength weighted by the wavenumber $1/\lambda$. Bis-ANS (4,4'-Dianilino-1,1'-Binaphthyl-5,5'-Disulfonic Acid) spectra (excitation 370nm, emission 400-600nm) were collected following a 2 minute incubation of 10 μM dye with 2 μM α_1-antitrypsin in PBS.

Molecular modeling

The mutation was modeled against the wild-type structure [1QLP (18)] using VMD (19) and NAMD (20) as described in the Supplementary text.

Thermal denaturation

The transition to the polymerization intermediate was monitored using a SYPRO Orange-based thermal denaturation assay as described previously (17), using various rates of temperature increase.

Polymerization kinetics monitored by FRET

The Cys232 residue of α_1-antitrypsin was labeled with Alexa Fluor 488 (AF488) maleimide and Alexa Fluor 594 (AF594) maleimide (Life Technologies). Polymerization was monitored as the increase in acceptor (AF594) fluorescence at 615nm with excitation of donor (AF488) at 470 nm using a Mastercycler realplex4 instrument (Eppendorf), as described (17, 21, 22).

Equilibrium unfolding/dilution refolding

Unfolding curves were obtained by incubating α_1-antitrypsin with guanidinium hydrochloride for 3 hours at room temperature, before recording intrinsic fluorescence spectra as described above. Derived COSM values were fitted to a three state unfolding model (23). Refolding involved denaturing a 10mg/ml stock of α_1-antitrypsin overnight at 4°C in 6M guanidinium hydrochloride, followed by rapid dilution into PBS containing 5% v/v glycerol to 0.05mg/ml, and resolution on a 3–12% w/v non-denaturing gel.

Results

Clinical case

A 41-year-old female, never-smoker of Iraqi origin was referred to the London Alpha-1 Antitrypsin Deficiency Service after her serum α_1-antitrypsin levels were measured at 0.4 g/L (normal range 1.0–2.8 g/L). She had been investigated for an ulnar neuropathy that resolved spontaneously. Family history revealed that her parents were first cousins. She reported no symptoms associated with α_1-antitrypsin deficiency. She was married to a third cousin with whom she had two children who are both alive and well. IEF phenotyping of circulating α_1-antitrypsin repeatedly produced an 'unclear result' (Supp. Fig. E1A). Standard liver function tests (including bilirubin, alkaline phosphatase, alanine transaminase, aspartate aminotransferase and γ-glutamyl transferase) were normal, albumin levels were marginally elevated, and there were no abnormalities on hepatic imaging by ultrasound or fibroscan. Lung function tests including spirometry and gas transfer indices were also normal. There was no abnormality of circulating anti-neutrophil cytoplasmic antibody (ANCA). In view of the circulating deficiency and unclear phenotyping, SERPINA1 genotyping was undertaken and identified homozygosity for a non-synonymous G1078C mutation, resulting in an Ala336Pro substitution that has not previously been described. This novel variant was named α_1-antitrypsin Baghdad (here also referred to as AT_{A336P}) after the birthplace of the index case.

Ala336Pro mutation occurs in a hot-spot for polymerogenic mutants and results in substantial polymerization in vivo

Ala336 is located centrally to strand 5 of β-sheet A (strand 5A, s5A) in α_1-antitrypsin in a region known as the 'shutter' (24) with a side-chain directed into the interior of the protein (Fig. 1A, *left panels*). Residues within this region are known to regulate the opening of β-sheet A for incorporation of the reactive centre loop as a neighboring strand (s4A) (25). Therefore, mutations in these residues can affect functional activity and the propensity to polymerize (24). In particular,

in the native conformation, Ala336 packs against Phe51, whose interactions contribute to the sheet-opening mechanism (26). Mutations at adjacent sites (Supp. Fig. E1B) result in highly polymerogenic variants of α_1-antitrypsin: S_{iiyama}, Ser53Pro (27); M_{malton} , Phe51del (28); and King's, His 336Asp (9). Accordingly, western blot analysis of patient plasma, separated by non-denaturing PAGE, indicated that the Baghdad variant was predominantly circulating as polymers that were recognized by the 2C1 monoclonal antibody. This indicates the Ala336Pro mutation results in polymers that share an epitope with pathological polymers of the Z variant that are observed *in vivo* (Fig. 1B, *right*).

Ala336Pro mutation reduces the inhibitory activity of α_1-antitrypsin

Monomeric AT_{A336P} α_1-antitrypsin was purified from plasma, and found to require a 2.7-fold greater stoichiometric excess (SI) over a model protease (α-chymotrypsin) than AT_M to achieve full inhibition (Table 1 and Fig. 1C). This reduction in activity is greater than that observed for AT_Z, and will increase the unproductive turnover of inhibitor, resulting in the release of RCL-cleaved serpin and active protease. This was confirmed by SDS-PAGE analysis of the interaction with α-chymotrypsin at twice the stoichiometry of inhibitor-to-enzyme. Consistent with the kinetic experiments, the amount of α_1-antitrypsin that formed complex with α-chymotrypsin relative to the cleaved, non-complexed protein, was lower for AT_{A336P} than for AT_Z (Supp. Fig. E1C). In addition to this decrease in the efficiency of protease inhibition due to increased unproductive turnover, the Ala336Pro mutation also reduced the rate of the interaction: the association rate constant (k_{ass}) was 13% that of AT_M (Table 1), lower than observed for Z α_1-antitrypsin (53% of AT_M). This suggests a sub-optimal RCL conformation for the encounter between α_1-antitrypsin and target protease. These deficits together with the reduction in circulating levels equates to a predicted *in situ* inhibitory rate that is two orders of magnitude slower for an Ala336Pro α_1-antitrypsin homozygote than for an M α_1-antitrypsin homozygote. This is comparable with the functional deficiency in Z α_1-antitrypsin homozygotes (Table 1, *right column*). In practice these values will significantly underestimate the loss-of-function for the deficiency variants as they do not account for the further reductions due to the proportion of α_1-antitrypsin circulating as functionally inactive polymers.

The proline substitution destabilizes β-sheet A by disrupting strand 5A-6A hydrogen bonds

The alanine-to-proline change represents a substitution that is predicted to alter local structure. While a bulkier side-chain may have some effect, it is an inherent restriction of backbone conformation that is expected to exert the greatest influence; proline residues are known act as 'strand-breakers' by disrupting the periodicity of the backbone angles inherent in these structural elements. To investigate the possibility of significant loss of secondary structure, circular dichroism spectra were recorded in the far-UV range. The substantially similar profile indicated a lack of change to the overall protein secondary structure, and thus a globally intact protein (Fig. 2A). However, differences were observed in the intrinsic tryptophan fluorescence spectrum of AT_{A336P} (Fig. 2B). In α_1-antitrypsin, the two tryptophan residues (Trp194 and Trp238) dominate the fluorescence profile, reporting changes in the breach region at the top of β-sheet A between s5A and s3A, and β-sheet B, respectively (29). The intensity of the AT_{A336P} spectrum was found to be intermediate between that of AT_M and AT_Z variants, with a 'red-shift' of the peak maximum in common with AT_Z. By analogy with AT_Z, this is highly likely to reflect differences in side-chain arrangements and an altered dynamic behavior that increases average solvent exposure in the vicinity of the breach of β-sheet A (30). This region is the site of the 'proximal' (N-terminal) hinge

of the RCL, and the compromised k_{ass} value noted for AT_{A336P} suggests the altered dynamics increase the proportion of molecules at a given time point with incompatible presentation of the protease recognition site. The environment-sensitive dye bis-ANS reports the presence of a hydrophobic binding site which coincides with the transition to a polymerization intermediate (31). This dye displays enhanced fluorescence in the presence of the AT_Z mutant (30), and yielded a comparable increase in AT_{A336P} fluorescence over that of AT_M (Fig. 2C), consistent with an increased population of the intermediate state.

The structural consequences of the Ala336Pro mutation on the conformation of the protein were investigated *in silico* using the NAMD (20) and VMD (19) packages. In the resulting model, the constraints imposed by the pyrrolidine ring of Pro336 do not disrupt strand 5A, consistent with a subset of backbone angles favored by proline residues that coincide with the β-sheet region of the Ramachandran plot. Indeed, it has been noted that proline residues can be accommodated in regions of a β-sheet that tolerate the disruption of the periodic main-chain hydrogen bonding, such as β-sheet edge strands (32). Consistent with this 'edge-strand-effect', the model predicts loss of two hydrogen bonds between strands 5A and 6A that partly disrupts the neighboring s6A backbone conformation (Fig. 1A, *right panels* and Supp. Figs. E1D and E1E). The s6A-helix I-s5A sequence forms a contiguous structural unit that abuts the site of RCL incorporation during conformational change, parts of which show enhanced exchange properties with the solvent in AT_Z (33). The effects on inhibitory activity suggest that the resulting reduction in β-sheet A stability is associated with changes in the conformational behavior of the RCL.

The native state is less stable in the mutant than wild-type

The centre of spectral mass (COSM), calculated from intrinsic fluorescence of α_1-antitrypsin under pseudo-equilibrium denaturing conditions, reflects changes in solvent exposure predominantly of Trp194 at low concentrations with an increasing contribution from Trp238 at higher concentrations (30). It thus largely represents a probe of breach conformational stability, which follows a three-state unfolding pathway (34) that can be summarized as follows:

$$\text{Predominantly closed (M-like)} \leftrightarrow \text{Open (Z-like)} \leftrightarrow \text{Unfolded}$$

Support for the scheme proposed here comes from similar red-shifted intrinsic spectral (30) and bis-ANS binding (34) properties for the M and Z α_1-antitrypsin variants in unfolding intermediate-inducing concentrations of denaturant (30).

Intrinsic protein fluorescence spectra were collected during pseudo-equilibrium unfolding of the three variants, and COSM values calculated. The resulting data were well-described by a three-state equation (Fig. 3A). The shapes of the plots show that an exposure of Trp194 characteristic of the intermediate state is already adopted by AT_Z. Native AT_{A336P} was found to be juxtaposed between AT_M and AT_Z, indicating the dynamic equilibrium shifted towards increased solvent exposure in the vicinity of the breach. The unfolding intermediates of AT_M and AT_{A336P} adopted a native Z-like COSM value, with the midpoints of the transitions indicating that AT_{A336P} adopts this state at a lower denaturant concentration than AT_M (Table 2). In contrast, the transition to the unfolded state was slightly earlier in AT_{A336P} than the other two variants. Together these data support a continued role for central strand 5A interactions in the denaturant-induced AT_M intermediate as it adopts Z-like dynamic behavior in the breach.

The loop-inserted conformation is less stable in the mutant than wild-type

Disruption of the integrity of β-sheet A by the introduction of a mid-strand proline might be expected to destabilize the loop-inserted conformation of α_1-antitrypsin. This hyperstable, thermodynamically-preferred state is achieved following cleavage of the RCL by a protease or partial misfolding to the latent form; additionally, the prevailing models of polymerization predicate a loop-inserted state for the repeating subunit. Protein, cleaved with *Staphylococcus aureus* protease V8 (35), was incubated in increasing concentrations of guanidinium hydrochloride for 2 hours, and resolved by PAGE using a 6M urea gel. This system preserved intact cleaved α_1-antitrypsin but prevented refolding of denatured protein on the gel. The resulting profile showed a transition for AT_{A336P} from folded to unfolded at 5.5 M guanidinium hydrochloride, a concentration approximately 0.5 M lower than that required to unfold cleaved AT_M and AT_Z (Fig. 3B). Thus, a destabilized β-sheet A manifests a decreased thermodynamic stability of the 6-stranded form.

The folding efficiency of Z α_1-antitrypsin is lower than that of the Ala336Pro variant

The α_1-antitrypsin variants were subjected to snap-refolding by a 200-fold dilution from a 10 mg/ml stock, and visualized by non-denaturing PAGE (Fig. 3C, *top panel*). The gels showed development of three conformations: monomer, a slower-migrating band reflecting the intermediate, and an oligomeric species likely to be dimer. Densitometry revealed the recovery of material to be incomplete on refolding, with 87.5%, 72.8% and 44.7% activity regained for AT_M, AT_{A336P} and AT_Z, respectively (Fig. 3C, lower panel). AT_{A336P} was therefore able to fold almost as well as AT_M, in contrast to AT_Z. Upon refolding, AT_{A336P} populated the intermediate state more than AT_M but less than AT_Z, whilst it formed the oligomeric state to a greater extent than either.

These observations, combined with the character of the intermediate in the presence of denaturant, indicate that Glu342 is foremost a 'gatekeeper' amino acid that is of particular importance in the folding pathway. However it is less important in preventing formation of ordered polymers associated with refolding. Conversely, the residues of the shutter are required for native stability and function, and the Ala336Pro mutation perturbs this to allow self-association after substantial refolding.

Ala336Pro allows the polymerization intermediate to form more readily than the Z mutation

Polymerization of α_1-antitrypsin can be induced by heat, yielding polymers that share an epitope with *ex vivo* material (9). Thermal challenge represents a tool for investigating the effect of a mutation on the polymerization pathway, which observes a progression from monomer native state (M) to a polymerization-prone monomeric intermediate (M*) that oligomerizes to form hyperstable polymers (P) (14, 17):

$$M \leftrightarrow M^* \ (+M^*) \rightarrow P$$

The native and intermediate states are considerably less thermodynamically stable than the polymeric form, to the extent that the polymerization step is essentially irreversible; consequently, techniques that interrogate this pathway observe a partially kinetic rather than an equilibrium process. Thermal denaturation experiments using SYPRO Orange involve an incremental increase

in temperature (typically 1°C min^{-1}), and provide a measure of the stability of the native state of a protein, reported as the temperature at which a 50% "unfolding" is observed (T_m). For α_1-antitrypsin, this reports the uni-molecular conversion from the native state to the polymerization intermediate (21).

This assay showed a general lack of reversibility when temperature was decreased following a period of heating (Supp. Fig. E1D). This reflected an inability of the system to achieve equilibrium, an effect that could be accounted for by varying the rate of temperature increase (36). Accordingly, the three variants were heated at increments of 0.5, 0.9, 1.4, 2.4, 3.2 and 9.0°C min^{-1} (rates determined *a posteriori* by measurement within the instrument during the experiment). The resulting T_m values were indeed influenced by the temperature ramp, confirming that the results are influenced by kinetic, rather than equilibrium processes (Fig. 4A, left panel). The apparent height of the energy barrier to intermediate formation, $E_{act,app}$ was derived from the slopes of the regressions (Fig. 4A, right panel). AT_Z was found to have a lower kinetic barrier (by 160±45 kJ mol^{-1}) to intermediate formation than AT_M, qualitatively consistent with results obtained for the rate of unfolding in denaturant (34), and for AT_{A336P} this was lower still (by 280±40 kJ mol^{-1}). Thus, AT_{A336P} is able to convert to the intermediate from the native state ($M \rightarrow M^*$) more readily than AT_Z or AT_M.

Ala336Pro increases the rate of polymerization

FRET (Förster resonance energy transfer) can be used to monitor the heat-induced incorporation of α_1-antitrypsin monomers into a growing polymer chain (17, 21, 22). The half-time of fluorescence increase was determined at a range of temperatures between 50-60°C (Fig. 4B, left panel). From a comparison of rates with AT_M and AT_Z on an Årrhenius plot (Fig. 4B, right panel), a downward shift was evident for AT_{A336P}. This reflects a considerably faster polymerization at all temperatures surveyed. The regression line permitted interpolation of a half-time at the median temperature of 55°C, at which AT_Z was found to polymerize 3.6 times and AT_{A336P} 21 times more quickly than AT_M (Fig. 4C, left panel).

Ala336Pro has specific effects on the polymerization mechanism

The slopes of the regression lines on the Årrhenius plot provide an indication of the energy barrier to oligomerization ($M^*+M^* \rightarrow P$) (17, 21). The values were found to be comparable for AT_M and AT_Z, but that of AT_{A336P} was considerably lower (Fig. 4C, right panel). Thus, in contrast to AT_Z, this mutation has effects on both phases of polymerization ($M \rightarrow M^*$ and $M^* + M^* \rightarrow P$).
We have previously reported a stability–polymerization profile that reflects the consensus relationship between the rate of polymerization and effects on native state stability (21). Deviations from this trend are diagnostic for specific effects of a mutation on the polymerization mechanism itself. Under the conditions of these experiments, this was found to be the case for both AT_Z and AT_{A336P} with respect to AT_M (Fig. 4D).

Discussion

Here we describe a novel mutant of α_1-antitrypsin in a homozygous individual who is healthy and has no personal or family medical history suggestive of α_1-antitrypsin deficiency. The comprehensive biophysical and biochemical characterization of the novel AT_{A336P} variant allows

detailed comparison with the classic AT_Z variant that is associated with severe lung and liver disease. This can be correlated with clinical chemistry findings, to inform her ongoing management and investigation and provide genetic counseling regarding the implications for her children; they are obligate carriers of at least one copy of the novel allele. The index individual has a profound functional deficiency of circulating AT_{A336P} due to multiple factors; in addition to reduced circulating levels of total α_1-antitrypsin in a range conventionally associated with moderate clinical significance, the protein is predominantly polymeric and the native monomer is far less effective as an antiprotease relative to the wild-type protein AT_M. The resultant loss-of-function is of similar severity to that observed in AT_Z (PiZZ) homozygotes.

Such 'experiments of nature' can also inform upon details of the mechanisms by which α_1-antitrypsin inhibits lung proteases in health and is subject to misfolding and polymerization in disease. The inhibitory mechanism involves translocation of a covalently bound protease by around 70 Å to the opposite pole of the molecule as the RCL becomes incorporated as additional strand within β-sheet A (s4A) (37). The Glu342Lys mutation in Z antitrypsin is situated in the 'breach' region of β-sheet A (Fig. 1A), which is the point of first incorporation for the RCL. Whilst the loss of the associated salt bridge has minimal consequences for the thermodynamic stability of the molecule (34), it is known that the result is a less efficient protease inhibitor than the wild-type protein reflected by a reduction in activity of around 30% (38). This suggests a defect in the mechanism of conformational change. Additionally, a decrease in the rate of association is observed, indicative of a non-native RCL presentation (13). The more pronounced perturbation of the inhibitory behavior by the Ala336Pro mutation – an SI of 2.7 and an SI-adjusted k_{ass} of 2.8×10^5 M^{-1} s^{-1} - similarly reflects the effects on β-sheet A and the conformation of the RCL, respectively, despite a location for the mutation that is 6 amino acids N-terminal to that of the Z allele. During the inhibitory process, helix F and the post-helix F loop represent a barrier that undergoes deformation in order to accommodate the translocating protease; these elements lie in the vicinity of Ala336 (39, 40). The thermodynamic destabilization of the inserted state (Fig. 3B) due to 'edge-strand-effects' (Fig. 1A, *right panels*) may reduce the energetic impetus that drives RCL insertion. This would provide an opportunity for the enzyme to become deacylated and escape the covalent complex.

Characterizing the folding of α_1-antitrypsin to a metastable native state, whether as a purified polypeptide or within cells, and misfolding in disease, are important research goals. Comparative refolding and equilibrium denaturant studies in AT_M, AT_Z and AT_{A336P} further inform on specifics of the process. Our observations suggest that Glu342 acts as a 'gatekeeper' residue, guiding the correct placement of the top of s5A in the folding intermediate, but that the nature of the residue at this position becomes far less important in thermodynamic stabilization of the native state. The central portion of s5A in contrast plays a more pronounced role in the native state than the intermediate, consistent with experiments using hydrogen-deuterium exchange that show this region to be in a slow exchange regimen, reflecting low conformational lability in AT_M (41).

The combination of low circulating α_1-antitrypsin levels and the observation that polymers of AT_{A336P} were present in the plasma of the affected individual, indicated that the novel mutation was polymerogenic. This was confirmed by characterization of the purified protein: reduced barriers to both intermediate formation and oligomerization were evident, rendering it more polymerization-prone than either AT_Z or AT_M. Whilst the thermodynamic stability of the native state of AT_Z is comparable to AT_M - with differences residing in the rate of interchange between native and unfolding intermediate – equilibrium denaturant and thermal unfolding showed the native and cleaved state of AT_{A336P} to be less stable than either (Fig. 3B, Fig. 3A and Fig. 4A, *left*). However both

AT_{A336P} and AT_Z predispose to polymerization by additional effects beyond global destabilization of the fold. They therefore act by specifically promoting conformational changes required for polymerization. The finding that folding and polymerization are differentially affected by Ala336Pro and Glu342Lys mutations indicates that the overall degree of misfolding and polymerization are not directly related in α_1-antitrypsin deficiency variants.

Challenge of monomeric α_1-antitrypsin by heat or denaturant results in polymers with different electrophoretic, immunological and structural characteristics (42, 43), but only the former share a conformational epitope with *ex vivo* pathological polymers (9, 42). It is likely that this difference is also manifest in intermediate ensembles induced by the two approaches. Indeed, the heat-induced α_1-antitrypsin intermediate shows evidence for a more compact state than that observed in 1M guanidinium hydrochloride (41, 42, 44). However, regional differences in s5A behavior are similar in both the denaturant-mediated and heat-induced polymerization (Table 2 and Fig. 4C, *right*). The Ala336Pro mutation influences stability of the denaturant-induced intermediate against further unfolding, and enhances the propensity of the thermal intermediate or refolded material to oligomerize. In contrast, the Glu342Lys mutation does not influence these steps.

The highly polymerogenic nature of the AT_{A336P} mutation clearly renders the homozygous individual more vulnerable to lung disease through loss-of-function. With regard to the liver disease, our detailed characterization of this protein allows us to place it into a class of mutants that exhibit similar properties. Specifically, its high propensity to polymerize, in common with neighboring shutter domain mutants associated with liver disease (45), indicates this individual should continue to be monitored for evidence of liver dysfunction. Thus insights from basic science, closely related to clinical context, are now guiding the personalized management of the AT_{A336P} α_1-antitrypsin homozygote.

(E) Acknowledgments

The authors thank the staff at the London Alpha-1 Antitrypsin Service for their help with this study.

(F) References

1. Zaimidou S, van Baal S, Smith TD, Mitropoulos K, Ljujic M, Radojkovic D, Cotton RG, Patrinos GP. A1ATVar: a relational database of human SERPINA1 gene variants leading to α1-antitrypsin deficiency and application of the VariVis software. *Human Mut* 2009;30:308-313.
2. Brantly ML, Wittes JT, Vogelmeier CF, Hubbard RC, Fells GA, Crystal RG. Use of a highly purified alpha 1-antitrypsin standard to establish ranges for the common normal and deficient alpha 1-antitrypsin phenotypes. *Chest* 1991;100:703-708.
3. Allan PC, Harley RA, Talamo RC. A new method for determination of alpha-1-antitrypsin phenotype using isoelectric focusing on polyacrylamide gel slabs. *Am J Clin Path* 1974;62:732-739.
4. Sveger T. Liver disease in alpha1-antitrypsin deficiency detected by screening of 200,000 infants. *N Engl J Med* 1976;294:1316-1321.
5. Silverman EK, Miletich JP, Pierce JA, Sherman LA, Endicott SK, Broze GJ, Jr., Campbell EJ. Alpha-1-antitrypsin deficiency. High prevalence in the St. Louis area determined by direct population screening. *Am Rev Respir Dis* 1989;140:961-966.
6. Qu D, Teckman JH, Omura S, Perlmutter DH. Degradation of a mutant secretory protein, α1-antitrypsin Z, in the endoplasmic reticulum requires proteasome activity. *J Biol Chem* 1996;271:22791-22795.
7. Lomas DA, Evans DL, Finch JT, Carrell RW. The mechanism of Z alpha 1-antitrypsin accumulation in the liver. *Nature* 1992;357:605-607.
8. Tan L, Dickens JA, Demeo DL, Miranda E, Perez J, Rashid ST, Day J, Ordonez A, Marciniak SJ, Haq I, Barker AF, Campbell EJ, Eden E, McElvaney NG, Rennard SI, Sandhaus RA, Stocks JM, Stoller JK, Strange C, Turino G, Rouhani FN, Brantly M, Lomas DA. Circulating polymers in alpha1-antitrypsin deficiency. *Eur Respir J* 2014;43:1501-1504.
9. Miranda E, Perez J, Ekeowa UI, Hadzic N, Kalsheker N, Gooptu B, Portmann B, Belorgey D, Hill M, Chambers S, Teckman J, Alexander GJ, Marciniak SJ, Lomas DA. A novel monoclonal antibody to characterize pathogenic polymers in liver disease associated with alpha1-antitrypsin deficiency. *Hepatology* 2010;52:1078-1088.
10. Mahadeva R, Lomas DA. Alpha1-antitrypsin deficiency, cirrhosis and emphysema. *Thorax* 1998;53:501-505.
11. Alam S, Li Z, Janciauskiene S, Mahadeva R. Oxidation of Z alpha1-antitrypsin by cigarette smoke induces polymerization: a novel mechanism of early-onset emphysema. *Am J Respir Cell Mol Biol* 2011;45:261-269.
12. Irving JA, Pike RN, Lesk AM, Whisstock JC. Phylogeny of the serpin superfamily implications of patterns of amino acid conservation for structure and function. *Genome Res* 2000;10:1845-1864.
13. Lomas DA, Evans DL, Stone SR, Chang WS, Carrell RW. Effect of the Z mutation on the physical and inhibitory properties of alpha 1-antitrypsin. *Biochemistry* 1993;32:500-508.
14. Dafforn TR, Mahadeva R, Elliott PR, Sivasothy P, Lomas DA. A kinetic mechanism for the polymerization of alpha1-antitrypsin. *J Biol Chem* 1999;274:9548-9555.
15. Schneider CA, Rasband WS, Eliceiri KW. NIH Image to ImageJ: 25 years of image analysis. *Nature Meth* 2012;9:671-675.
16. Laemmli UK. Cleavage of structural proteins during the assembly of the head of bacteriophage T4. *Nature* 1970;227:680-685.
17. Haq I, Irving JA, Faull SV, Dickens JA, Ordonez A, Belorgey D, Gooptu B, Lomas DA. Reactive centre loop mutants of alpha-1-antitrypsin reveal position-specific effects on intermediate formation along the polymerization pathway. *Biosci Rep* 2013;33.

18. Elliott PR, Abrahams JP, Lomas DA. Wild-type alpha 1-antitrypsin is in the canonical inhibitory conformation. *J Mol Biol* 1998;275:419-425.
19. Humphrey W, Dalke A, Schulten K. VMD: visual molecular dynamics. *J Mol Graph* 1996;14:33-38, 27-38.
20. Phillips JC, Braun R, Wang W, Gumbart J, Tajkhorshid E, Villa E, Chipot C, Skeel RD, Kalé L, Schulten K. Scalable molecular dynamics with NAMD. *J Comp Chem* 2005;26:1781-1802.
21. Irving JA, Haq I, Dickens JA, Faull SV, Lomas DA. Altered native stability is the dominant basis for susceptibility of alpha1-antitrypsin mutants to polymerization. *Biochem J* 2014;460:103-115.
22. Irving JA, Miranda E, Haq I, Perez J, Kotov VR, Faull SV, Motamedi-Shad N, Lomas DA. An antibody raised against a pathogenic serpin variant induces mutant-like behaviour in the wild-type protein. *Biochem J* 2015;461:99-108.
23. Barrick D, Baldwin RL. Three-state analysis of sperm whale apomyoglobin folding. *Biochemistry* 1993;32:3790-3796.
24. Stein PE, Carrell RW. What do dysfunctional serpins tell us about molecular mobility and disease? *Nat Struct Biol* 1995;2:96-113.
25. Whisstock JC, Skinner R, Carrell RW, Lesk AM. Conformational changes in serpins: I. The native and cleaved conformations of alpha(1)-antitrypsin. *J Mol Biol* 2000;295:651-665.
26. Kwon KS, Kim J, Shin HS, Yu MH. Single amino acid substitutions of alpha 1-antitrypsin that confer enhancement in thermal stability. *J Biol Chem* 1994;269:9627-9631.
27. Lomas DA, Finch JT, Seyama K, Nukiwa T, Carrell RW. Alpha 1-antitrypsin Siiyama (Ser53-->Phe). Further evidence for intracellular loop-sheet polymerization. *J Biol Chem* 1993;268:15333-15335.
28. Lomas D, Elliott P, Sidhar S, Foreman R, Finch J, Cox D, Whisstock J, Carrell R. alpha 1-Antitrypsin Mmalton (Phe52-deleted) forms loop-sheet polymers in vivo. Evidence for the C sheet mechanism of polymerization. *J Biol Chem* 1995;270:16864-16870.
29. Tew DJ, Bottomley SP. Probing the equilibrium denaturation of the serpin alpha(1)-antitrypsin with single tryptophan mutants; evidence for structure in the urea unfolded state. *J Mol Biol* 2001;313:1161-1169.
30. Knaupp AS, Bottomley SP. Structural change in beta-sheet A of Z alpha(1)-antitrypsin is responsible for accelerated polymerization and disease. *J Mol Biol* 2011;413:888-898.
31. James EL, Whisstock JC, Gore MG, Bottomley SP. Probing the unfolding pathway of alpha1-antitrypsin. *J Biol Chem* 1999;274:9482-9488.
32. MacArthur MW, Thornton JM. Influence of proline residues on protein conformation. *J Mol Biol* 1991;218:397-412.
33. Hughes VA, Meklemburg R, Bottomley SP, Wintrode PL. The Z Mutation alters the global structural dynamics of α1-antitrypsin. *PLoS ONE* 2014;9:e102617.
34. Knaupp AS, Levina V, Robertson AL, Pearce MC, Bottomley SP. Kinetic instability of the serpin Z α1-antitrypsin promotes aggregation. *J Mol Biol* 2010;396:375-383.
35. Lomas DA, Elliott PR, Chang WS, Wardell MR, Carrell RW. Preparation and characterization of latent alpha 1-antitrypsin. *J Biol Chem* 1995;270:5282-5288.
36. Sánchez-Ruiz JM, López-Lacomba JL, Cortijo M, Mateo PL. Differential scanning calorimetry of the irreversible thermal denaturation of thermolysin. *Biochemistry* 1988;27:1648-1652.
37. Huntington JA, Read RJ, Carrell RW. Structure of a serpin-protease complex shows inhibition by deformation. *Nature* 2000;407:923-926.
38. Ogushi F, Fells GA, Hubbard RC, Straus SD, Crystal RG. Z-type alpha 1-antitrypsin is less competent than M1-type alpha 1-antitrypsin as an inhibitor of neutrophil elastase. *J Clin Invest* 1987;80:1366-1374.

39. Cabrita LD, Dai W, Bottomley SP. Different conformational changes within the F-helix occur during serpin folding, polymerization, and proteinase inhibition. *Biochemistry* 2004;43:9834-9839.
40. Maddur AA, Swanson R, Izaguirre G, Gettins PGW, Olson ST. Kinetic intermediates en route to the final serpin-protease complex: STUDIES OF COMPLEXES OF α1-PROTEASE INHIBITOR WITH TRYPSIN. *J Biol Chem* 2013;288:32020-32035.
41. Tsutsui Y, Dela Cruz R, Wintrode PL. Folding mechanism of the metastable serpin α1-antitrypsin. *Proc Natl Acad Sci USA* 2012;109:4467-4472.
42. Ekeowa UI, Freeke J, Miranda E, Gooptu B, Bush MF, Perez J, Teckman J, Robinson CV, Lomas DA. Defining the mechanism of polymerization in the serpinopathies. *Proc Natl Acad Sci USA* 2010;107:17146-17151.
43. Yamasaki M, Li W, Johnson DJ, Huntington JA. Crystal structure of a stable dimer reveals the molecular basis of serpin polymerization. *Nature* 2008;455:1255-1258.
44. Tsutsui Y, Kuri B, Sengupta T, Wintrode PL. The structural basis of serpin polymerization studied by hydrogen/deuterium exchange and mass spectrometry. *J Biol Chem* 2008;283:30804-30811.
45. Janciauskiene S, Eriksson S, Callea F, Mallya M, Zhou A, Seyama K, Hata S, Lomas D. Differential detection of PAS-positive inclusions formed by the Z, Siiyama, and Mmalton variants of alpha1-antitrypsin. *Hepatology* 2004;40:1203-1210.
46. DeLano W. The PyMOL molecular graphics system, Version 1.3r1. 1.3r1 ed: Schrodinger; 2010.
47. Costas M, Rodriguez-Larrea D, De Maria L, Borchert TV, Gomez-Puyou A, Sanchez-Ruiz JM. Between-species variation in the kinetic stability of TIM proteins linked to solvation-barrier free energies. *J Mol Biol* 2009;385:924-937.

(G) Footnotes

(H) Tables

Table 1. *The effect of the Ala336Pro mutation on protease inhibition*

Stoichiometries of inhibition (SI) and association rate constants (k_{ass}) were determined against bovine α-chymotrypsin at 25°C. Standard errors are calculated from three independent experiments.

Variant	SI*	k_{ass} (M^{-1} s^{-1})	k_{ass}•S.I (M^{-1} s^{-1})	Notional rate†
AT_M	1.0	2.65±0.13 x 10^5	2.65 x 10^5	100%
AT_Z	1.5	0.93±0.10 x 10^5	1.40 x 10^5	3.5%
AT_{A336P}	2.7	0.13±0.03 x 10^5	0.35 x 10^5	1.0%

* Standard errors were less than 5%.

† Calculated as the rate of inhibition (in s^{-1}) relative to AT_M at a typical concentration (2, 0.2 and 0.4 mg/ml for AT_M, AT_Z, and AT_{A336P} respectively) if this were entirely circulating as native monomer.

Table 2. *Equilibrium unfolding transition midpoints of α_1-antitrypsin variants*

The midpoints of denaturation (in guanidium hydrochloride) were obtained by fitting a function describing three-state unfolding to the equilibrium denaturation profiles in Fig. 3A. The standard errors of the fits are shown.

	Midpoint (GdnHCl M)	
Variant	**N→I**	**I→U**
AT_M	0.94±0.03	2.43±0.03
AT_Z	1.33±0.09	2.43±0.06
$AT_{Ala336Pro}$	0.42±0.04	2.27±0.03

(J) Figure Legends

Figure 1. Characteristics of patient derived α_1-antitrypsin. (A) *Left panels*: Structure cartoon of the wild-type protein [accession 1QLP (18)] generated using PyMol (46) showing the position of Ala336 in the standard β-sheet A ("A-sheet") view and rotated counterclockwise by 90°, with the reactive centre loop ("RCL") indicated. Sheets A, B and C are colored red, pink and yellow, respectively. *Right panels*: An energy-minimized molecular model of AT_{A336P} compared with the wild-type coordinates treated in the same manner using NAMD (20) and VMD (19). The arrows indicate the loss of two main-chain hydrogen bonds (depicted as hatched lines) in the model between strands 5A and 6A. (B) Western blot analysis of patient derived plasma from MM, ZZ and Ala336Pro/Ala336Pro homozygotes separated by 3–12% w/v non-denaturing PAGE with detection by rabbit polyclonal ("Total") and polymer-specific ("2C1") antibodies. Higher order bands represent polymeric species. The AT_{A336P} polymer is recognized by 2C1, demonstrating the presence of an epitope shared with the Z polymer. (C) Calculation of the SI of α_1-antitrypsin variants against bovine α-chymotrypsin, showing residual activity at different ratios of inhibitor to enzyme. Error bars denote standard deviations from three experiments.

Figure 2. Structural features of Ala336Pro. (A) Assessment of overall secondary structure by far-UV circular dichroism (CD). CD spectra of plasma-derived α_1-antitrypsin, at 0.5 mg/ml in 10 mM Na_2HPO_4/NaH_2PO_4 pH7.4, recorded between 250-190 nm, show similar profiles for the three variants. (B) Assessment of breach opening (30) by intrinsic tryptophan fluorescence. Spectra were recorded of 0.5 μM α_1-antitrypsin in PBS with 5% v/v glycerol between 300-400 nm with excitation at 295 nm. Ala336Pro shows increased fluorescence intensity and red shift in wavelength compared to AT_M, however, to a lesser extent than AT_Z α_1-antitrypsin. (C) 2 μM α_1-antitrypsin in PBS with 5% v/v glycerol was incubated with 10 μM bis-ANS for 10 minutes and the spectra recorded between 400-600 nm with excitation at 370 nm. The increase in fluorescence was comparable to AT_Z, suggesting increased population of the polymerization intermediate (34).

Figure 3. Equilibrium unfolding and rapid refolding of α_1-antitrypsin. (A) Changes in intrinsic fluorescence centre of spectral mass (COSM) during equilibrium unfolding of 0.5 μM α_1-antitrypsin are shown. Values calculated at 6 M guanidinium hydrochloride were similar to those at 4 M. Samples were in 10 mM Na_2HPO_4/NaH_2PO_4, pH7.4. (B) AT_M, AT_Z and AT_{A336P} were cleaved overnight at a 50-fold molar excess with respect to *Staphylococcus aureus* protease V8, and incubated for 2 hours in increasing concentrations of guanidinium hydrochloride before separation by 6 M urea PAGE. In each 8% acrylamide gel, native and cleaved protein in the absence of denaturant (left two lanes) were used as controls. Unfolding of the protein resulted in a decreased rate of migration. This shift in behavior occurred at a lower concentration for AT_{A336P} than the other variants. (C) *Top:* 1 μg of α_1-antitrypsin was concentrated to 10mg/ml in PBS with 5% v/v glycerol, *C*, or in 6 M guanidinium hydrochloride, *R*, before 200 fold dilution into PBS with 5% v/v glycerol. Samples were resolved on a 3–12% w/v non-denaturing gel stained with Coomassie Brilliant Blue. M, I and P represent the positions of monomer, intermediate and polymer fractions respectively (42). *Bottom:* Analysis of refolding by densitometry. Each bar represents the total protein regained on refolding compared to the control, *C*, samples. Demarcation of the bars represents the proportion of conformer regained.

Figure 4. The effects of Ala336Pro on thermal stability. (A) *Left*: Conversion of AT_M, AT_Z and AT_{A336P} variants from native to intermediate upon heating between 25°C and 95°C was monitored in PBS using SYPRO Orange dye (21), and the midpoint of the thermal transition, T_m, plotted as a

function of rate of temperature increase (47). *Right*: the calculated apparent activation energy values, $E_{act,app}$, for the transition between native and intermediate states, calculated from the slopes of the regressions. (B) *Left:* AT_{A336P}, labeled with Alexa 488 and Alexa 594 dyes at Cys232 in equimolar ratios, was heated over a range of temperatures at 0.1 mg/ml in PBS and the increase in FRET monitored. Typical results of an experiment are shown (solid black lines), with curves of best fit (dashed grey lines). *Right*: Half-times of polymerization of AT_{A336P} were determined from FRET progress curves at a range of temperatures and subjected to an Årrhenius analysis (17, 21). (C) *Left*: the Årrhenius plot was used to interpolate a polymerization half-time for the variants at a single reference temperature (55°C). The polymerization of AT_{A336P} was faster than for either AT_Z or AT_M variants. *Right*: the apparent activation energy for polymerization, $E_{act,app}$, was calculated from the Årrhenius plot. This was significantly lower for AT_{A336P} than either the AT_M or AT_Z variants, as judged by a one-way ANOVA ($p<0.05$). (D) Half-times of polymerization at 55°C and the T_m values of the AT_Z and AT_{A336P} variants are shown relative to that of AT_M. The dashed lines represent a consensus relationship between a rate of polymerization dictated by native state stability (21).

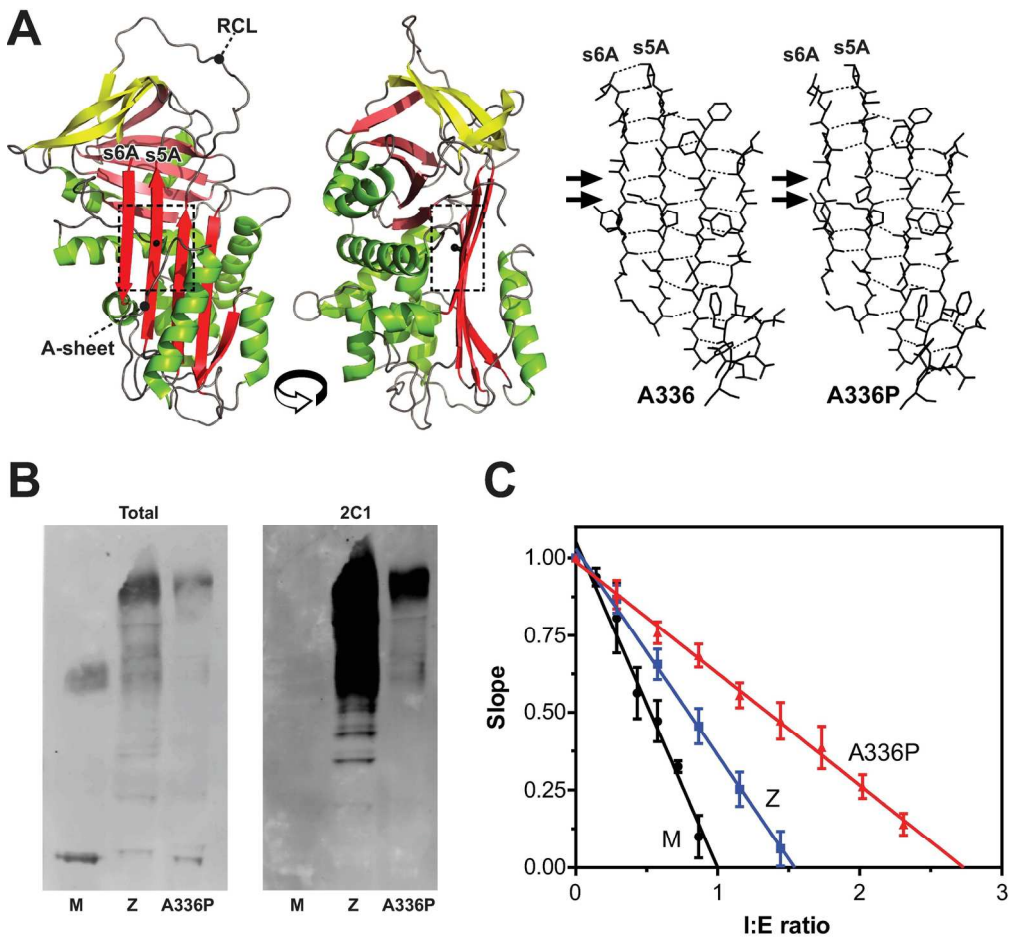

Figure 1. Characteristics of patient derived α_1-antitrypsin. (A) *Left panels*: Structure cartoon of the wild-type protein [accession 1QLP (18)] generated using PyMol (46) showing the position of Ala336 in the standard β-sheet A ("A-sheet") view and rotated counterclockwise by 90°, with the reactive centre loop ("RCL") indicated. Sheets A, B and C are colored red, pink and yellow, respectively. *Right panels*: An energy-minimized molecular model of AT_{A336P} compared with the wild-type coordinates treated in the same manner using NAMD (20) and VMD (19). The arrows indicate the loss of two main-chain hydrogen bonds (depicted as hatched lines) in the model between strands 5A and 6A. (B) Western blot analysis of patient derived plasma from MM, ZZ and Ala336Pro/Ala336Pro homozygotes separated by 3–12% w/v non-denaturing PAGE with detection by rabbit polyclonal ("Total") and polymer-specific ("2C1") antibodies. Higher order bands represent polymeric species. The AT_{A336P} polymer is recognized by 2C1, demonstrating the presence of an epitope shared with the Z polymer. (C) Calculation of the SI of α_1-antitrypsin variants against bovine α-chymotrypsin, showing residual activity at different ratios of inhibitor to enzyme. Error bars denote standard deviations from three experiments.
165x154mm (300 x 300 DPI)

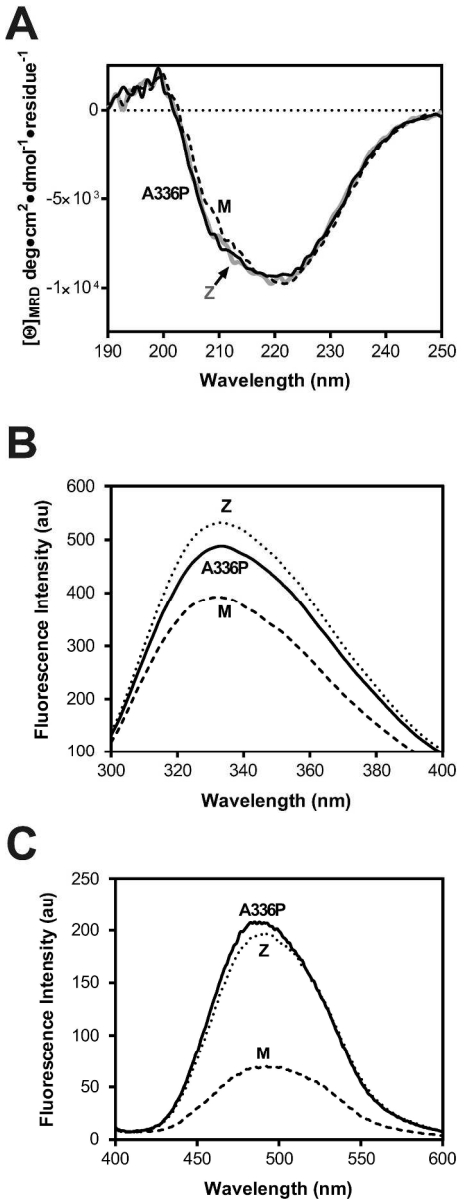

Figure 2. Structural features of Ala336Pro. (A) Assessment of overall secondary structure by far-UV circular dichroism (CD). CD spectra of plasma-derived α_1-antitrypsin, at 0.5 mg/ml in 10 mM Na_2HPO_4/NaH_2PO_4 pH7.4, recorded between 250-190 nm, show similar profiles for the three variants. (B) Assessment of breach opening (30) by intrinsic tryptophan fluorescence. Spectra were recorded of 0.5 μM α_1-antitrypsin in PBS with 5% v/v glycerol between 300-400 nm with excitation at 295 nm. Ala336Pro shows increased fluorescence intensity and red shift in wavelength compared to AT_M, however, to a lesser extent than AT_Z α_1-antitrypsin. (C) 2 μM α_1-antitrypsin in PBS with 5% v/v glycerol was incubated with 10 μM bis-ANS for 10 minutes and the spectra recorded between 400-600 nm with excitation at 370 nm. The increase in fluorescence was comparable to AT_Z, suggesting increased population of the polymerization intermediate (34).
222x373mm (300 x 300 DPI)

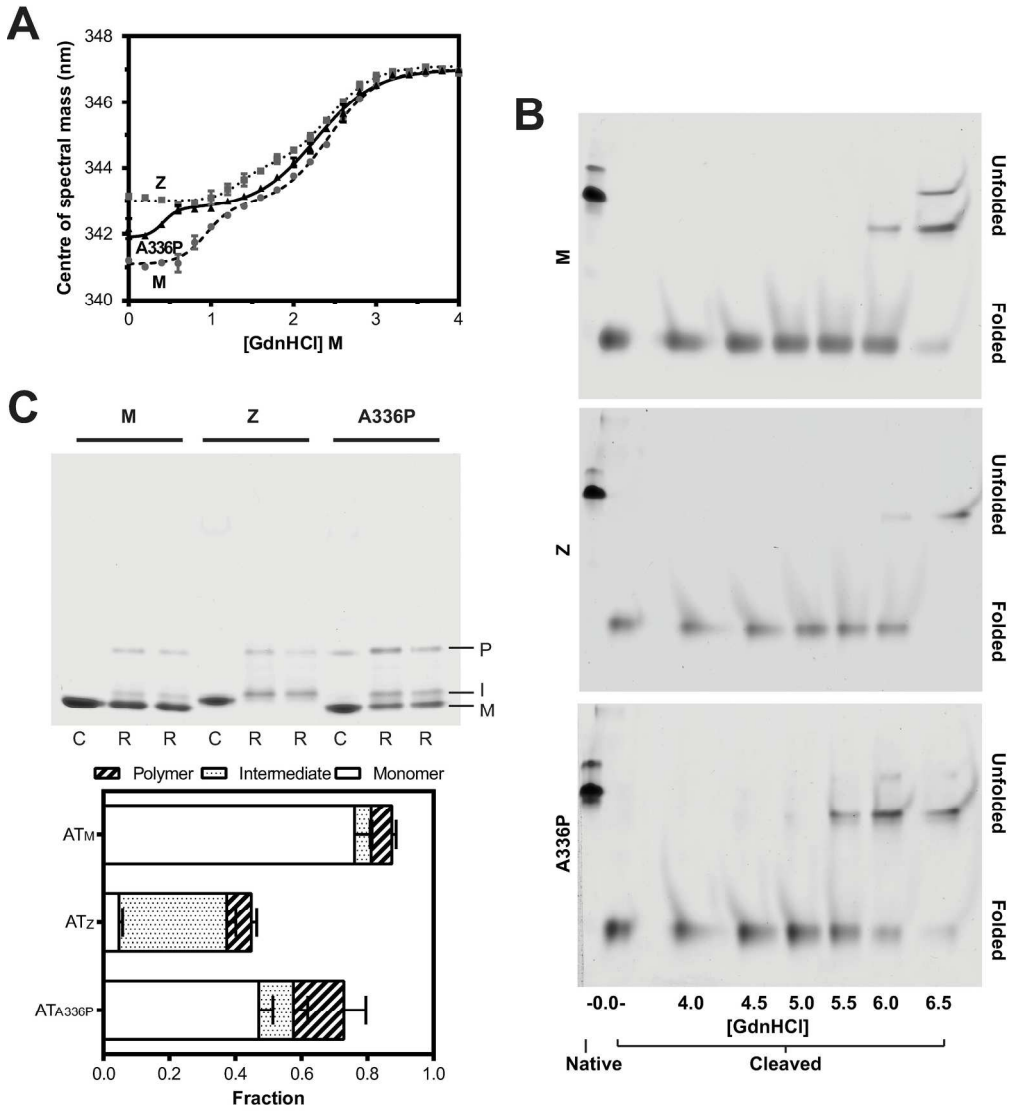

Figure 3. Equilibrium unfolding and rapid refolding of α_1-antitrypsin. (A) Changes in intrinsic fluorescence centre of spectral mass (COSM) during equilibrium unfolding of 0.5 μM α_1-antitrypsin are shown. Values calculated at 6 M guanidinium hydrochloride were similar to those at 4 M. Samples were in 10 mM Na_2HPO_4/NaH_2PO_4, pH7.4. (B) AT_M, AT_Z and AT_{A336P} were cleaved overnight at a 50-fold molar excess with respect to *Staphylococcus aureus* protease V8, and incubated for 2 hours in increasing concentrations of guanidinium hydrochloride before separation by 6 M urea PAGE. In each 8% acrylamide gel, native and cleaved protein in the absence of denaturant (left two lanes) were used as controls. Unfolding of the protein resulted in a decreased rate of migration. This shift in behavior occurred at a lower concentration for AT_{A336P} than the other variants. (C) *Top:* 1 μg of α_1-antitrypsin was concentrated to 10mg/ml in PBS with 5% v/v glycerol, *C*, or in 6 M guanidinium hydrochloride, *R*, before 200 fold dilution into PBS with 5% v/v glycerol. Samples were resolved on a 3–12% w/v non-denaturing gel stained with Coomassie Brilliant Blue. M, I and P represent the positions of monomer, intermediate and polymer fractions respectively (42). *Bottom:* Analysis of refolding by densitometry. Each bar represents the total protein regained on refolding compared to the control, *C,* samples. Demarcation of the bars represents the proportion of conformer regained.

207x229mm (300 x 300 DPI)

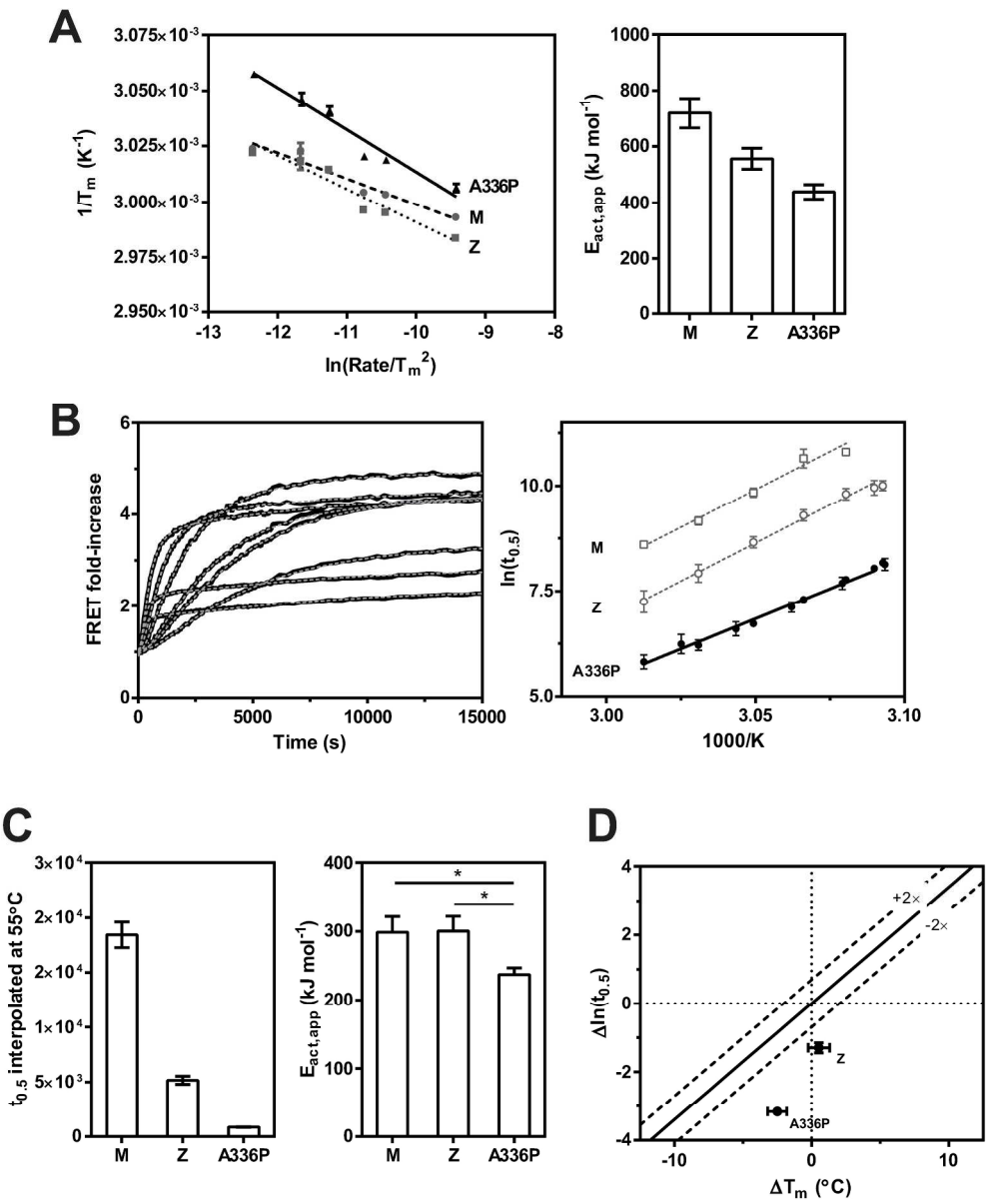

Figure 4. The effects of Ala336Pro on thermal stability. (A) *Left*: Conversion of AT_M, AT_Z and AT_{A336P} variants from native to intermediate upon heating between 25°C and 95°C was monitored in PBS using SYPRO Orange dye (21), and the midpoint of the thermal transition, T_m, plotted as a function of rate of temperature increase (47). *Right*: the calculated apparent activation energy values, $E_{act,app}$, for the transition between native and intermediate states, calculated from the slopes of the regressions. (B) *Left:* AT_{A336P}, labeled with Alexa 488 and Alexa 594 dyes at Cys232 in equimolar ratios, was heated over a range of temperatures at 0.1 mg/ml in PBS and the increase in FRET monitored. Typical results of an experiment are shown (solid black lines), with curves of best fit (dashed grey lines). *Right*: Half-times of polymerization of AT_{A336P} were determined from FRET progress curves at a range of temperatures and subjected to an Årrhenius analysis (17, 21). (C) *Left*: the Årrhenius plot was used to interpolate a polymerization half-time for the variants at a single reference temperature (55°C). The polymerization of AT_{A336P} was faster than for either AT_Z or AT_M variants. *Right*: the apparent activation energy for polymerization, $E_{act,app}$, was calculated from the Årrhenius plot. This was significantly lower for AT_{A336P} than either the AT_M or AT_Z variants, as

judged by a one-way ANOVA ($p<0.05$). (D) Half-times of polymerization at 55°C and the T_m values of the AT_Z and AT_{A336P} variants are shown relative to that of AT_M. The dashed lines represent a consensus relationship between a rate of polymerization dictated by native state stability (21).
223x271mm (300 x 300 DPI)

Supplemental material

Materials and Methods

Molecular modeling of the A336P mutation

The crystal structure of α_1-antitrypsin [PDB accession 1QLP (E1)] was the basis for molecular dynamics simulations, with VMD (E2) and NAMD (E3) used for preparation/visualization and minimization/molecular dynamics, respectively. The system was prepared for production molecular dynamics in the following way: (a) the alanine-to-proline mutation at position 336 was introduced; (b) hydrogens were added, the structure was placed in a water box with 1 nm borders, and the overall charge neutralized using sodium ions; (c) the solvent and protein hydrogens were minimized with the protein non-hydrogen atoms fixed for 10k cycles; (d) the protein was minimized with the solvent fixed for 10k cycles; and (e) both were minimized together for 10k cycles. A 5 ns production molecular dynamics run at 37°C was performed, with snapshots taken at 0.5 ps intervals. The resulting model was obtained as follows: (a) the root-mean-square deviation of Cα atoms was calculated relative to the starting structure; (b) the snapshots were averaged across the stable portion of the molecular dynamics trajectory, starting at round 0.4 ns; and (c) a final found of energy minimization of 2.5k cycles was performed. This process was also performed for the wild-type protein.

Supplementary Figure E1. (A) Portion of the isoelectric focusing gel that yielded an inconclusive result for the Ala336Pro/Ala336Pro homozygote ("sample"). The positions of bands corresponding to Z and S alleles are indicated. (B) 'Cut-through' figure showing the atomic packing of Ala336 (colored red) relative to the sites of other shutter domain mutations, shaded grey. (C) 2μg of each α_1-antitrypsin variant was incubated with bovine α-chymotrypsin at a 1:1 molar ratio to active monomer in chymotrypsin assay buffer for 15 min at room temperature. Samples were mixed with SDS loading buffer without boiling and separated by 4-12% w/v SDS-PAGE, and visualized by Coomassie Brilliant Blue. The gel shows the ability of all variants to form SDS-stable serpin-enzyme complex. P indicates protease alone, A indicates α_1-antitrypsin alone and C indicates protease incubated with α_1-antitrypsin; the positions of covalent complex (with and without secondary cleavage), intact and non-productively cleaved α_1-antitrypsin and α-chymotrypsin are also indicated. (D) Molecular dynamics simulation with wild-type ("A336A") and mutant ("A336P") models was performed at 37°C with sampling at 0.5 ps intervals. $RMSD_{ref}$ denotes the root-mean-square deviation of Cα atoms with respect to the starting models, and show stabilization of the trajectory at around 0.4 ns. (E) Cartoon representation of the molecular model of AT_{A336P}, highlighting the predicted disruption of strand 6A by the Ala336Pro mutation. (F) AT_M at 0.1 mg/ml in PBS was heated from 25°C to 55°C and cooled back to 25°C at a rate of 5°C min^{-1}, with conformational change monitored using SYPRO Orange. The profile shows a lack of reversibility of the transition upon cooling.

References

E1. Elliott PR, Abrahams JP, Lomas DA. Wild-type alpha 1-antitrypsin is in the canonical inhibitory conformation. *J Mol Biol* 1998;275:419-425.

E2. Humphrey W, Dalke A, Schulten K. VMD: visual molecular dynamics. *J Mol Graph* 1996;14:33-38, 27-38.

E3. Phillips JC, Braun R, Wang W, Gumbart J, Tajkhorshid E, Villa E, Chipot C, Skeel RD, Kalé L, Schulten K. Scalable molecular dynamics with NAMD. *J Comp Chem* 2005;26:1781-1802.

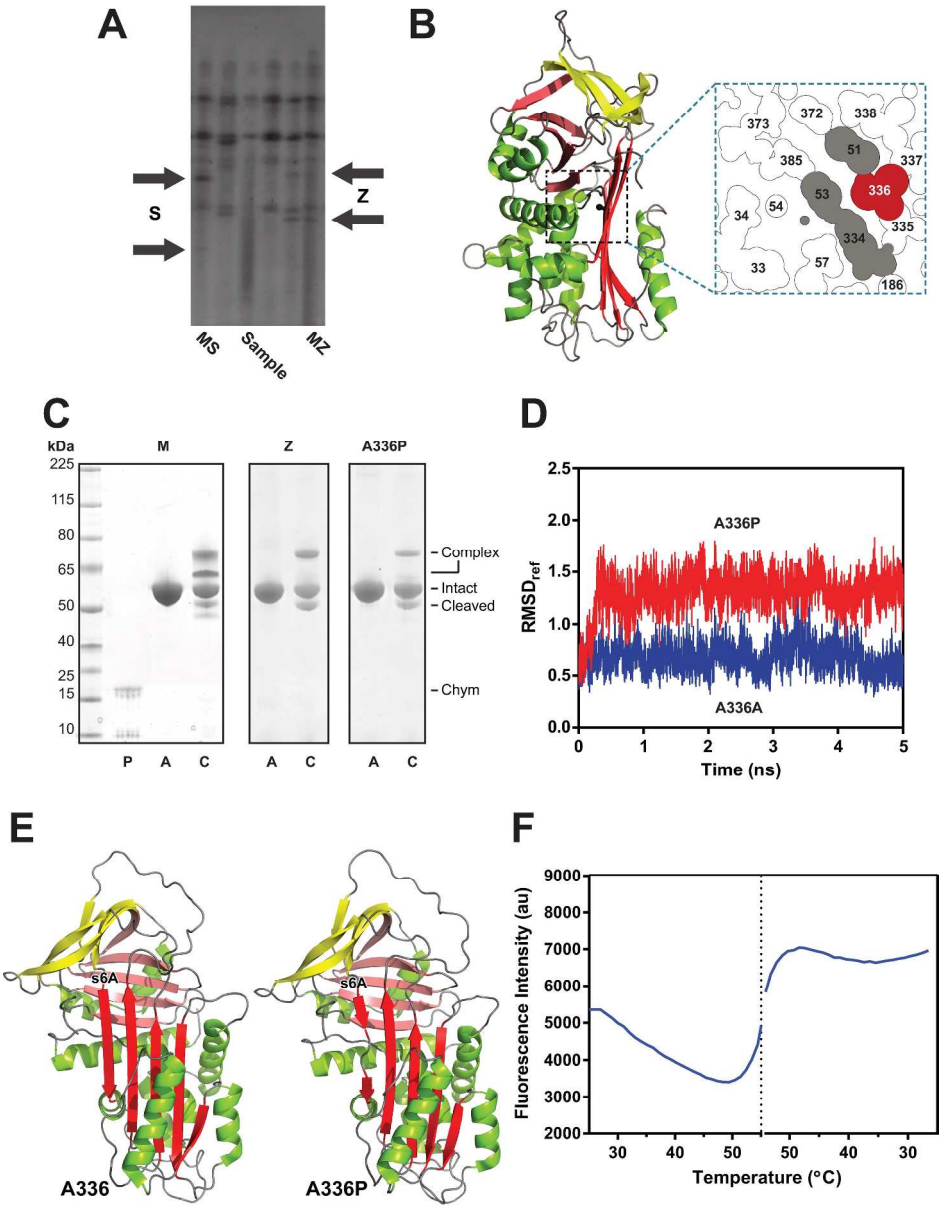

Supplementary Figure E1. (A) Portion of the isoelectric focusing gel that yielded an inconclusive result for the Ala336Pro/Ala336Pro homozygote ("sample"). The positions of bands corresponding to Z and S alleles are indicated. (B) 'Cut-through' figure showing the atomic packing of Ala336 (colored red) relative to the sites of other shutter domain mutations, shaded grey. (C) 2μg of each α_1-antitrypsin variant was incubated with bovine α-chymotrypsin at a 1:1 molar ratio to active monomer in chymotrypsin assay buffer for 15 min at room temperature. Samples were mixed with SDS loading buffer without boiling and separated by 4-12% w/v SDS-PAGE, and visualized by Coomassie Brilliant Blue. The gel shows the ability of all variants to form SDS-stable serpin-enzyme complex. P indicates protease alone, A indicates α_1-antitrypsin alone and C indicates protease incubated with α_1-antitrypsin; the positions of covalent complex (with and without secondary cleavage), intact and non-productively cleaved α_1-antitrypsin and α-chymotrypsin are also indicated. (D) Molecular dynamics simulation with wild-type ("A336A") and mutant ("A336P") models was performed at 37°C with sampling at 0.5 ps intervals. $RMSD_{ref}$ denotes the root-mean-square deviation of Cα atoms with respect to the starting models, and show stabilization of the trajectory at around 0.4 ns. (E)

Cartoon representation of the molecular model of AT_{A336P}, highlighting the predicted disruption of strand 6A by the Ala336Pro mutation. (F) AT_M at 0.1 mg/ml in PBS was heated from 25°C to 55°C and cooled back to 25°C at a rate of 5°C min^{-1}, with conformational change monitored using SYPRO Orange. The profile shows a lack of reversibility of the transition upon cooling.
249x320mm (300 x 300 DPI)